This is the accepted version of the publication Yin, R., Tao, X. M., & Xu, B. G. (2018). Variation of false twist on spinning process stability and resultant yarn properties in a modified ring spinning frame. In Textile Research Journal (Vol. 88, Issue 16, pp. 1876–1892) Copyright © The Author(s) 2017. DOI: 10.1177/0040517517712099.

Variation of False Twist on Spinning Process Stability and Resultant Yarn Properties in a Modified Ring Spinning Frame

R. Yin, X. M. Tao & B. G. XU
Institute of Textiles and Clothing, The Hong Kong Polytechnic University, Hong Kong
E-mail: xiao-ming.tao@polyu.edu.hk

Abstract
Twisting is an important process to form a continuous yarn from short fibres and to determine the structure and properties of the resultant yarn. This article reports on the effect of variation of false twist on process stability and resultant yarn quality in a modified ring spinning frame. Based on twist kinematics, three practical cases that cause twist variations in spinning process are investigated, namely step function, rectangular function and periodic function changes in false twist. The simulation results are validated by experiments and a good agreement has been demonstrated. The resultant properties of yarn within 30% periodic change in false twist demonstrated insignificance compared with yarn without variation. With the developed model, essential system parameters are numerically examined and their quantitative relationships are studied. The practical implications are discussed.

Keywords: yarn twist, yarn properties, twist variation, twist kinematics, false twist

Symbol lists

$N_b = v_b / 2\pi R_0$ - Yarn theoretical rotational speed by belt without yarn slippage (rev/sec)
ΔN_b - Amplitude of belt speed variation (res/sec)
N_t - Traveler rotational speed (rev/sec)
n_b - Yarn rotational acceleration (rev/sec^2)
n_t - Traveler rotational acceleration (rev/sec^2)
λ - Belt twisting efficiency
η - Coefficient of belt twist congestion
k - Coefficient of belt twist trapping
T_c - Actual false twist generated by the belt (turns/m)
T_h - Twist increment in zone OA due to the congestion effect (turns/m)
T_t - Twist trapped by the belt (turns/m)
T_B - Twist generated by traveler (turns/m)
T_1 - False twist in zone OA at time t (turns/m)
T_2 - False twist in zone AB at time t (turns/m)
T_3 - False twist in zone BC at time t (turns/m)
$\mathbf{T_1}$ - Yarn twist in zone OA at time t (turns/m)
$\mathbf{T_2}$ - Yarn twist in zone AB at time t (turns/m)
$\mathbf{T_3}$ - Yarn twist in zone BC at time t (turns/m)
l_1 - Length of zone OA (m)
l_2 - Length of zone AB (m)
l_3 - Length of zone BC (m)
v - Yarn delivery speed (m/sec)

v_b - Belt moving speed (m/sec)
d - Yarn diameter (m)
R_0 - Yarn radius (m)
t - Time (second)
ω - Angular frequency of belt speed variation (rad/sec)
f - Frequency of belt speed variation (Hz)

1 Introduction

Spinning is a fundamental method to impart strength and make continuous yarns by twisting short or staple fibers.[1] The yarns are then woven or knitted into fabrics for apparel and home-textile applications, where cotton, wool or man-made synthetic fibers are used.[2] With an output of 41,021,976 tons produced from all fibers and world cotton consumption of 23,633,845 tons in 2012, spun yarns show the dramatic swell of global textiles and apparel industry in the past decades.[3] In terms of the spinning technologies, ring spinning is the most dominating method since it can produce high quality yarn and has a wide spinnability to majority fiber materials and yarn counts.[4]

Based on the conventional ring spinning method, a modified technique has been proposed for producing a low residue torque and soft handle singles yarn by introducing a friction-belt false-twister.[5] Due to the incorporating of the false-twister, twist distributions in the yarn spinning zone are altered. In the upstream of the false-twister, a high twist level is achieved by combined twist coming from the false-twister and twist propagation through the false-twister from the traveler, which modifies the geometry of spinning triangle and greatly influences the distribution of fiber tension forces and fiber arrangements in a yarn, resulting in modified yarn structure and properties; while in the downstream of the false-twister, a low twist yarn is obtained by adopting a low twist factor, which results in a low residue torque and soft handle style. Structural analysis revealed that in the modified cotton ring yarns, most internal fibers have much lower inclination angles and some fiber segments have the inclination angle of alternating direction, thus yielding a reduced resultant contribution to the total yarn torque. Besides, the modified cotton yarns have a densely packed zone which is located in somewhere half way from the centre to the surface of the yarn thus the yarn of low twist can still hold itself with a reasonable tenacity and exhibit good pilling performance. Comparative studies [4, 6-9] have demonstrated that the modified cotton yarns and fabrics have significant advantages in terms of soft handle, higher yarn strength at lower twist factor, lower residual torque and low knitted fabric spirality after washing and tumble-dry cycles.

Twisting is an important process to form a continuous yarn and to determine the structure and properties of the resultant yarn. [10] Uniform twists inserted into the yarn ensure even features and good yarn quality. Twist variation in the spinning process may results in poor spinnability as well as uneven features or imperfections of the resultant yarns, such as strength deterioration, diameter irregularity and wrapping fibers along yarn length. On the other hand, for a stable process or product, it should permit a certain tolerance for the system variation or error. In the past decades, investigation of the twisting process has attracted interest by many researchers in the fields of ring spinning [11-14], rotor spinning [15, 16], friction spinning [17, 18], self-twist spinning [19-22], air-jet spinning [23, 24], etc. In particular, Fraser et al [25] studied the effect of yarn non-uniformity in the ring spinning process, and quantified that even a slub that in practice would be considered quite small can have a significant effect on the stability of the yarn balloon. Denton [26] investigated the effects of twisting-rate variations in the false-twist-texturing process and demonstrated that an oscillating twisting rate can generate an amplitude of twist in the downstream zones greater than the original variation in the texturing zone. Thus, it is of great concern that whether the system which combines the ring spinning and false twisting methods is stable or not, however little work on this novel topic could be found in the literature.

Apparently, it is important to develop a theoretical model to describe the effect of false twist variations on the yarn twist redistributions in the spinning process as well as evaluation of the yarn quality subject to external perturbations. Therefore, in this paper, equations are derived to evaluate the twist variations subject to external perturbations based on twist kinematics.[26-28] The model is then verified by the experimental observations and yarn properties subject to the variation of false twist are examined. The main purpose of this study is to assess the stability and robustness of the modified technique as well as comprehending the effect of system parameters on dynamical twist redistributions.

2 The Modified Ring Spinning System

As shown in Figure 1, a translationally moving belt was introduced into the conventional ring spinning frame and installed between the front rollers and yarn guide. In the modified spinning system, there are two twisters: one is the real-twister at point B; another is the false-twister which generates the torque by the frictional moment at point A. Correspondingly, the yarn path can be divided into three zones: zone OA between the front rollers and the false-twister (l_1); zone AB between the false-twister and the traveler (l_2); and zone BC between the traveler and the winding point (l_3). The winding point is also called wind-on or lay point, where it is wound onto the bobbin carried on the spindle which is coaxial with the ring. During the spinning process, the yarn moves at a constant velocity v, but its twist level is altered in different zones.

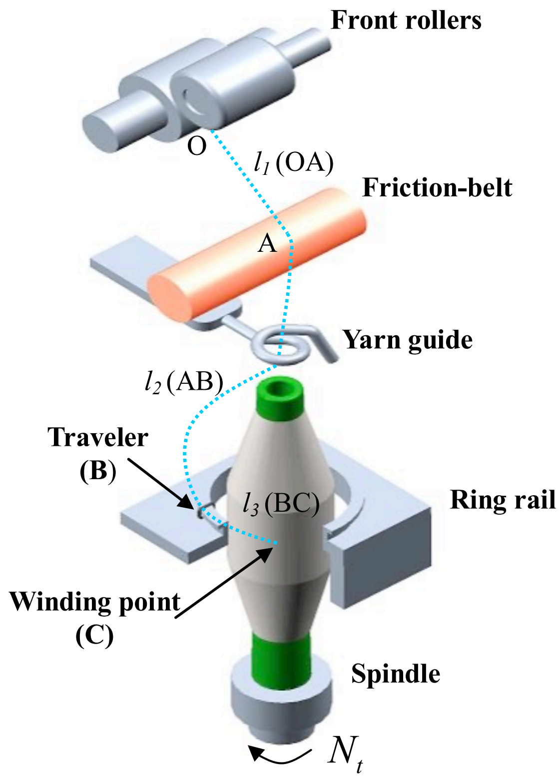

Figure 1 A schematic diagram of a modified ring spinning system

In order to describe the function played by the moving belt, three parameters are introduced. The first parameter is the false-twisting efficiency of the moving belt. At the contacting area of the yarn surface and the moving belt, the frictional moment forces the yarn to rotate along its axis. If there is no slippage or jumping of the yarn on the moving belt, then the yarn's tangential velocity and the moving velocity of the belt at the contacting point should be the same. In this situation, the false-twisting efficiency of the moving belt is unity, but normally the false-twisting efficiency is a value close to but below the unity. The false-twisting efficiency of the moving belt is expressed as

$$\lambda = \frac{2\pi R_0 T_c v}{v_b} \tag{1}$$

The second effect is the twist trapping in the up-ward propagation of the real twist inserted by the traveler. Without the existence of the belt, the yarn twist generated by the traveler can be freely propagated into zone OA. Due to the introduction of the moving belt, a certain proportion of this twist is blocked because of the frictional moment generated at point A. To quantify this effect, the propagation coefficient of twist trapping is defined as

$$k = 1 - \frac{T_t}{T_B} \tag{2}$$

The last effect is the twist congestion, which occurs in the downward propagation of twist in zone OA. The downward travelling yarn has a twist thus a tendency to untwist on the belt. It is subject to another frictional moment, as a result, the rotating trend of the yarn is reduced, which blocks the yarn twist propagating into zone AB. The result is that the yarn twist is increased in zone OA. The propagation coefficient of the twist congestion is defined as

$$\eta = \frac{T_c}{T_c + T_h} \tag{3}$$

3 Theoretical Modeling

3.1 Assumptions

The following assumptions are made to simplify the theoretical modeling:

(1) Twist distribution in each zone is regarded as linear superposition of twists from the traveler and the false-twister;

(2) Yarn slippage rate on moving belt, coefficient of belt twist congestion and trapping are constant throughout;

(3) The effects of twist blockage caused by the yarn guide and the traveler are neglected;

(4) The effects of twist-contraction in each zone are neglected;

(5) The twist is evenly distributed in each zone.

(6) The yarn delivery speed is constant in each of the three zones.

3.2 Twist distributions in the steady-state

From the kinematic point of view, the twist in zone OA can be expressed as

$$\mathbf{T}_1 = \frac{kN_t}{v} + \frac{\lambda N_b}{\eta v} \tag{4}$$

In zone AB, the friction-belt inserts turns into the yarn at the same rate as in zone OA, but in the opposite sense, which offsets the positive twist passing from zone OA. Therefore, the twist in zone AB in the steady-state is

$$\mathbf{T}_2 = \frac{N_t}{v} \tag{5}$$

In zone BC, no turns will be generated in this section and the twist in zone BC remains the same as that in zone AB

$$\mathbf{T}_3 = \frac{N_t}{v} \tag{6}$$

3.3 Twist redistributions in the transient-state

In some occurrences, yarn twist in three zones are altered due to the temporary or transient change of false twist such as variation of the belt moving speed, variation of the wrap angle of the belt and the yarn, and variation of yarn diameter. For easy derivation and experimental implementation, the change of belt moving speed is adopted for instance. In terms of the mode of variations, three functions are commonly used, namely step function, rectangular function, and periodic function. In this study, the periodic variation of the false twist is of particular interest because it meets the most practical applications, while the other two modes are also derived in the Appendix. In the transient-state, twist redistributions vary with time due to the altered false twist by changing the belt moving speed, while the real twist remains unchanged. As mentioned above, the twist redistribution in each zone is the linear superposition of real-twist and false-twist. Therefore, the total twist in each zone is the sum of the unchanged real twist and altered false twist.

The impact on the development of twist redistribution by false twist variations during nominally steady-state running is of much great practical interest. Hence, equations are developed that describes the way in which twists in the three zones of a modified ring spinning machine alter by a sinusoidal change in belt twisting rate. In this example, the belt twisting rate is given by the expression $N_b + \Delta N_b \sin \omega t$, where $\omega = 2\pi f$ in the usual way.

False Twist in Zone OA

The turns gained by the moving belt in a time increment dt are $\lambda(N_b + \Delta N_b \sin \omega t)dt$, the turns lost through the belt are $\eta T_1 v dt$, and the net twists gained are $dT_1 = \frac{\lambda(N_b + \Delta N_b \sin \omega t) - \eta T_1 v}{l_1} dt$, integration of which together with the initial condition $t = 0$, $T_1 = \frac{\lambda N_b}{\eta v}$, gives

$$T_1 = \frac{\lambda N_b}{\eta v} + \frac{\lambda \Delta N_b}{l_1}\left(A\left(\exp\left(-\frac{\eta v}{l_1} t \right) - \cos(\omega t) \right) + B \sin(\omega t) \right) \tag{7}$$

where $A = \frac{\omega}{\left(\frac{\eta v}{l_1} \right)^2 + \omega^2}$, $B = \frac{\frac{\eta v}{l_1}}{\left(\frac{\eta v}{l_1} \right)^2 + \omega^2}$

False Twist in Zone AB

The turns passing through the belt from Zone OA are $\eta T_1 v dt$, the negative turns inserted by the moving belt are $-\lambda(N_b + \Delta N_b \sin \omega t)dt$, and the turns passing through the traveler are $T_2 v dt$, so the net twists gained are $dT_2 = \frac{\eta T_1 v - \lambda(N_b + \Delta N_b \sin \omega t) - T_2 v}{l_2} dt$, integration of which and rearranging, together with the initial condition $t = 0$, $T_2 = 0$, gives

$$T_2 = \frac{\lambda \eta A \Delta N_b}{l_1 - \eta l_2}\left(\exp(-\frac{\eta v}{l_1} t) - \exp(-\frac{v}{l_2} t) \right) - \frac{\lambda \eta v A \Delta N_b}{l_1 l_2}\left(C\left(\cos(\omega t) - \exp\left(-\frac{v}{l_2} t \right) \right) + D \sin(\omega t) \right)$$
$$+ \frac{(\eta v B - l_1)\lambda \Delta N_b}{l_1 l_2}\left(D\left(\exp\left(-\frac{v}{l_2} t \right) - \cos(\omega t) \right) + C \sin(\omega t) \right) \tag{8}$$

where $C = \frac{\frac{v}{l_2}}{\left(\frac{v}{l_2} \right)^2 + \omega^2}$, $D = \frac{\omega}{\left(\frac{v}{l_2} \right)^2 + \omega^2}$

False Twist in Zone BC

The turns passing through the traveler from Zone AB be $T_2 v dt$, the turns wound onto the bobbin be $T_3 v dt$, so the net twists gained be $dT_3 = \frac{T_2 v - T_3 v}{l_3} dt$, integration of which and rearranging, together with the initial condition $t = 0$, $T_3 = 0$, gives

$$T_3 = \frac{\lambda\eta A l_1 \Delta N_b}{(l_1-\eta l_2)(l_1-\eta l_3)}\left(\exp\left(-\frac{\eta v}{l_1}t\right)-\exp\left(-\frac{v}{l_3}t\right)\right)-\frac{\lambda\eta A l_2 \Delta N_b}{(l_1-\eta l_2)(l_2-l_3)}\left(\exp\left(-\frac{v}{l_2}t\right)-\exp\left(-\frac{v}{l_3}t\right)\right)$$
$$-\frac{\lambda\eta v^2 A\Delta N_b}{l_1 l_2 l_3}\left((CE-DF)\left(\cos(\omega t)-\exp\left(-\frac{v}{l_3}t\right)\right)+(CF+DE)\sin(\omega t)-\frac{C l_2 l_3}{v(l_2-l_3)}\left(\exp\left(-\frac{v}{l_2}t\right)-\exp\left(-\frac{v}{l_3}t\right)\right)\right)$$
$$+\frac{(\eta v B-l_1)\lambda v\Delta N_b}{l_1 l_2 l_3}\left(-(CF+DE)\left(\cos(\omega t)-\exp\left(-\frac{v}{l_3}t\right)\right)+(CE-DF)\sin(\omega t)+\frac{D l_2 l_3}{v(l_2-l_3)}\left(\exp\left(-\frac{v}{l_2}t\right)-\exp\left(-\frac{v}{l_3}t\right)\right)\right) \quad (9)$$

where $E=\dfrac{\frac{v}{l_3}}{\left(\frac{v}{l_3}\right)^2+\omega^2}$, $F=\dfrac{\omega}{\left(\frac{v}{l_3}\right)^2+\omega^2}$

Therefore, yarn total twists in each zone can be expressed by the

$$\mathbf{T_1} = \frac{kN_t}{v}+\frac{\lambda N_b}{\eta v}+\frac{\lambda\Delta N_b}{l_1}\left(A\left(\exp\left(-\frac{\eta v}{l_1}t\right)-\cos(\omega t)\right)+B\sin(\omega t)\right) \quad (10)$$

$$\mathbf{T_2} = \frac{N_t}{v}+\frac{\lambda\eta A\Delta N_b}{l_1-\eta l_2}\left(\exp(-\frac{\eta v}{l_1}t)-\exp(-\frac{v}{l_2}t)\right)-\frac{\lambda\eta v A\Delta N_b}{l_1 l_2}\left(C\left(\cos(\omega t)-\exp\left(-\frac{v}{l_2}t\right)\right)+D\sin(\omega t)\right)$$
$$+\frac{(\eta v B-l_1)\lambda\Delta N_b}{l_1 l_2}\left(D\left(\exp\left(-\frac{v}{l_2}t\right)-\cos(\omega t)\right)+C\sin(\omega t)\right) \quad (11)$$

$$\mathbf{T_3} = \frac{N_t}{v}+\frac{\lambda\eta A l_1 \Delta N_b}{(l_1-\eta l_2)(l_1-\eta l_3)}\left(\exp\left(-\frac{\eta v}{l_1}t\right)-\exp\left(-\frac{v}{l_3}t\right)\right)-\frac{\lambda\eta A l_2 \Delta N_b}{(l_1-\eta l_2)(l_2-l_3)}\left(\exp\left(-\frac{v}{l_2}t\right)-\exp\left(-\frac{v}{l_3}t\right)\right)$$
$$-\frac{\lambda\eta v^2 A\Delta N_b}{l_1 l_2 l_3}\left((CE-DF)\left(\cos(\omega t)-\exp\left(-\frac{v}{l_3}t\right)\right)+(CF+DE)\sin(\omega t)-\frac{C l_2 l_3}{v(l_2-l_3)}\left(\exp\left(-\frac{v}{l_2}t\right)-\exp\left(-\frac{v}{l_3}t\right)\right)\right)$$
$$+\frac{(\eta v B-l_1)\lambda v\Delta N_b}{l_1 l_2 l_3}\left(-(CF+DE)\left(\cos(\omega t)-\exp\left(-\frac{v}{l_3}t\right)\right)+(CE-DF)\sin(\omega t)+\frac{D l_2 l_3}{v(l_2-l_3)}\left(\exp\left(-\frac{v}{l_2}t\right)-\exp\left(-\frac{v}{l_3}t\right)\right)\right) \quad (12)$$

Transforming equations (10-12) into the dimensionless form, one obtains

$$\overline{\mathbf{T_1}} = k+\frac{\lambda\overline{N_b}}{\eta}+\frac{\lambda\overline{\Delta N_b}}{\overline{l_1}}\left(\overline{A}\left(\exp\left(-\frac{\eta}{\overline{l_1}}\overline{t}\right)-\cos\left(\overline{\omega t}\right)\right)+\overline{B}\sin\left(\overline{\omega t}\right)\right) \quad (13)$$

$$\overline{\mathbf{T_2}} = 1+\frac{\lambda\eta\overline{A}\overline{\Delta N_b}}{\overline{l_1}-\eta\overline{l_2}}\left(\exp(-\frac{\eta}{\overline{l_1}}\overline{t})-\exp(-\frac{1}{\overline{l_2}}\overline{t})\right)-\frac{\lambda\eta\overline{A}\overline{\Delta N_b}}{\overline{l_1}\overline{l_2}}\left(\overline{C}\left(\cos(\overline{\omega t})-\exp\left(-\frac{1}{\overline{l_2}}\overline{t}\right)\right)+\overline{D}\sin(\overline{\omega t})\right)$$
$$+\frac{(\eta\overline{B}-\overline{l_1})\lambda\overline{\Delta N_b}}{\overline{l_1}\overline{l_2}}\left(\overline{D}\left(\exp\left(-\frac{1}{\overline{l_2}}\overline{t}\right)-\cos(\overline{\omega t})\right)+\overline{C}\sin(\overline{\omega t})\right) \quad (14)$$

$$\overline{\mathbf{T}_3} = 1 + \frac{\lambda\eta\overline{A}\overline{l_1}\overline{\Delta N_b}}{(\overline{l_1}-\eta\overline{l_2})(\overline{l_1}-\eta)}\left(\exp\left(-\frac{\eta}{\overline{l_1}}\overline{t}\right)-\exp\left(-\overline{t}\right)\right)-\frac{\lambda\eta\overline{A}\overline{l_2}\overline{\Delta N_b}}{(\overline{l_1}-\eta\overline{l_2})(\overline{l_2}-1)}\left(\exp\left(-\frac{1}{\overline{l_2}}\overline{t}\right)-\exp\left(-\overline{t}\right)\right)$$
$$-\frac{\lambda\eta\overline{A}\overline{\Delta N_b}}{\overline{l_1}\overline{l_2}}\left((\overline{C}\overline{E}-\overline{D}\overline{F})\left(\cos(\overline{\omega}\overline{t})-\exp\left(-\overline{t}\right)\right)+(\overline{C}\overline{F}+\overline{D}\overline{E})\sin(\overline{\omega}\overline{t})-\frac{\overline{C}\overline{l_2}}{\overline{l_2}-1}\left(\exp\left(-\frac{1}{\overline{l_2}}\overline{t}\right)-\exp\left(-\overline{t}\right)\right)\right)$$
$$+\frac{(\eta\overline{B}-\overline{l_1})\lambda\overline{\Delta N_b}}{\overline{l_1}\overline{l_2}}\left(-(\overline{C}\overline{F}+\overline{D}\overline{E})\left(\cos(\overline{\omega}\overline{t})-\exp\left(-\overline{t}\right)\right)+(\overline{C}\overline{E}-\overline{D}\overline{F})\sin(\overline{\omega}\overline{t})+\frac{\overline{D}\overline{l_2}}{\overline{l_2}-1}\left(\exp\left(-\frac{1}{\overline{l_2}}\overline{t}\right)-\exp\left(-\overline{t}\right)\right)\right) \tag{15}$$

where $\overline{t}=\frac{vt}{l_3}$, $\overline{l_1}=\frac{l_1}{l_3}$, $\overline{l_2}=\frac{l_2}{l_3}$, $\overline{T_1}=\frac{vT_1}{N_t}$, $\overline{T_2}=\frac{vT_2}{N_t}$, $\overline{T_3}=\frac{vT_3}{N_t}$, $\overline{\Delta N_b}=\frac{\Delta N_b}{N_t}$, $\overline{\omega}=\frac{\omega l_3}{v}$
$\overline{A}=\frac{vA}{l_3}$, $\overline{B}=\frac{vB}{l_3}$, $\overline{C}=\frac{vC}{l_3}$, $\overline{D}=\frac{vD}{l_3}$, $\overline{E}=\frac{vE}{l_3}$, $\overline{F}=\frac{vF}{l_3}$, $\overline{f}=\frac{fl_3}{v}$

4 Experimental Verification

4.1 Experimental setup

The experiments were conducted on a ring spinning frame (Zinser 351) by installing a Polyurethane belt with diameter of 3 mm between the front rollers and the yarn guide. The belt was driven by a 0.75 kw AC motor (NERI MOTORI) and the belt speed was controlled by a 220V single-phase inverter (Shanghai JINQV Automation Ltd., Co.; Model:VFD-V-2S0007B). The online control of the instant belt moving speed was accomplished by the embedded PLC module. In order to monitor the instant belt speed, a Hall speed sensor (SHANG HAI CE ZHEN AUTOMATION INSTRUMENT Co., LTD; Model:Y62) was adopted to measure the gear with 50 teeth attached to a belt pulley. For this study, yarn twists in both high twist zone and final state were measured and compared with theoretical predictions. In order to measure the instant twist in high twist zone, a black and unstained combed roving (count 332 g/km, measured CV of 4.32%, and fiber specifications: fiber length 1.475 inch, fiber strength 32.5 g/tex, uniformity ratio 54.53%, elongation 6.53% and micronaire value 4.35) were fed without gap into the back rollers of the ring spinning machine to produce yarn with linear density of 18.45 g/km (32Ne) and diameter of 0.164 mm for measurement. High-speed photography was applied for continual and automatic image acquisition, storage and analysis of yarn instant twist including a high-speed camera (Phantom MIRO 4, CMOS sensor, 800 x 600 pixels, over 1200 fps at full resolution, 22 μm pixel size, 12-bit depth), which was connected to a personal computer installed with camera control software and Nikon micro lens (AF Micro-Nikkor 60 mm f/2.8D). [29] The belt speed and the yarn twist in OA zone were collected synchronously for model verification. The final yarn twist was measured by untwist-retwist method (ASTM D1422-99) for qualitative analysis. In addition, the yarn properties such as tenacity, evenness, wet snarlings and hairiness were tested and compared with control yarns.

4.2 Experimental design

As shown in Table 1, the divided zone lengths for OA, AB and BC were set at 73, 327, and 20 mm, respectively. The wrap angle of the belt and yarn was fixed at 50°, and the twist factor for the yarn Ne 32 was 3.2, and the yarn delivery speed was 0.257 m/s. The traveler weight for the yarn was 35 mg and the frictional coefficient of the yarn and moving belt was 0.81 measured. The belt twisting efficiency, propagation coefficients of twist trapping and congestion were calculated 0.11, 0.88 and 0.90, respectively.[10]

Table 1 System parameters

l_1 (mm)	l_2 (mm)	l_3 (mm)	φ (°)	v (m/s)	α_e	m_w (mg)	μ	λ	k	η
73	327	20	50	0.257	3.2	35	0.81	0.11	0.88	0.90

According to our online twist measurement based on the high-speed photography, the twist variation for the conventional yarn in the spinning zone is 15-20% due to roving unevenness, error of the twist measurement, uneven distributions of yarn twist, etc. Therefore, in order to measure the yarn twist in OA zone, variation of the false twist should be chosen at a high level, which could suppress the noise caused by the aforementioned factors. In this study, we set speed ratio $v_b / v = 1.5$, amplitude of 1.5 with three frequency levels of 0.5 Hz, 0.2 Hz, and 0.1 Hz and then compare the experimental results with the theoretical model. For yarn properties evaluation, such large twist variation is not likely the case and of less practical interests, thus the following values were used for measuring the yarn properties and final yarn twists: speed ratio of 1.5, amplitude of 0.15, and frequency level of 0.5 Hz. The control yarn without belt speed variation was produced as a benchmark for comparison.

4.3 Calibration

As shown in Figure 2, high-speed photography technique was applied to capture images of yarn twist, and the system is composed of a high-speed camera, a light source and tripod frames. The tripod frame of the high-speed camera was used to locate the direction of camera lens perpendicular to the yarn profile, which ensures the precision of the measurement. The light was used for providing sufficient illumination during the shooting process.

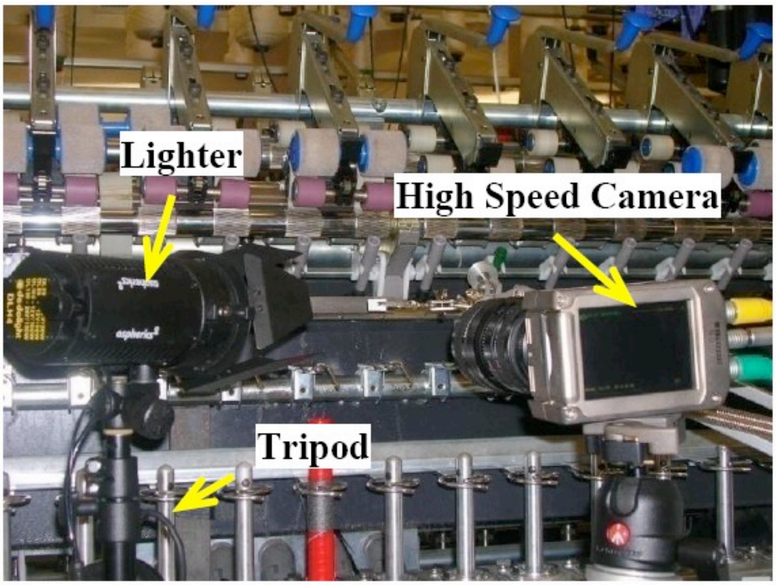

Figure 2 A high-speed photography system

In order to obtain the twist from images, a black-white yarn was adopted. One black and unstained rovings with the similar count were fed into the back rollers simultaneously. As a result of twisting, the bundle of straight and parallel fibers was laid along the helix curve on the yarn surface, and yarn twist could be directly read by the interval of black and white fiber bundles. A scale paper of 1 mm x 1 mm size was put beneath the yarn to calculate the real length of one twist turn, as shown in Figure 3. The yarn twist can be derived by $T=1/h$, where T represents the number of twist turns per unit length, h is the length of one turn of twist. Sixty images were used for the computation of yarn twist at each boundary. And for each image, three readings were extracted, generating 180 raw data.

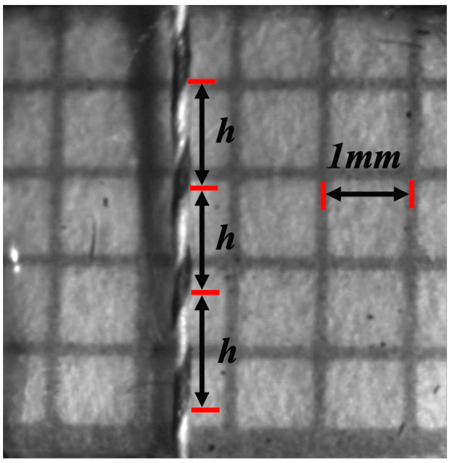

Figure 3 Determination of yarn twist from image

Before measurement of the twist, the high-speed camera system was calibrated. Six twist levels were used for calibration and images of the twist were captured under a resolution of 512 × 512 pixels with a sampling frequency of 1000 frames per second.

The measured values were compared with the results by using standard testing method ASTM D1423-02. As shown in Figure 4, twist measured by the high-speed photography method is approximately linear against the benchmark results by the standard method, which implies that the high-speed photography method can provide adequate accuracy and reliability for twist measurement. The relationship can be expressed by the linear regression equation as

$$Y=0.915X+9.018 \tag{16}$$

The correlation coefficient is 0.999.

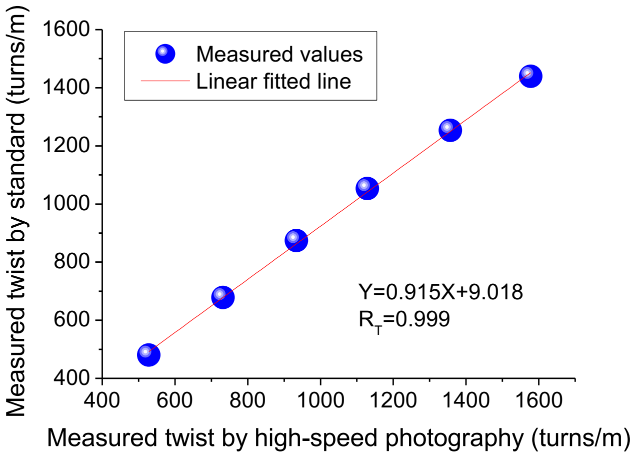

Figure 4 Calibration of yarn twist

Similarly, the Hall speed sensor must be calibrated before online measurement of belt speed. The output signal corresponding to the rotating speed is analogy current ranging from 4-20 mA. After calculation, the relationship between output current and belt speed ratio was found. In the calibration process, six speed ratios were tested and the results are shown in Figure 5. The measuring value covers all the operational range in the experiment and the results can be expressed by the linear regression formula as

$$Y=2.401X+4.089 \tag{17}$$

The correlation coefficient is 0.999.

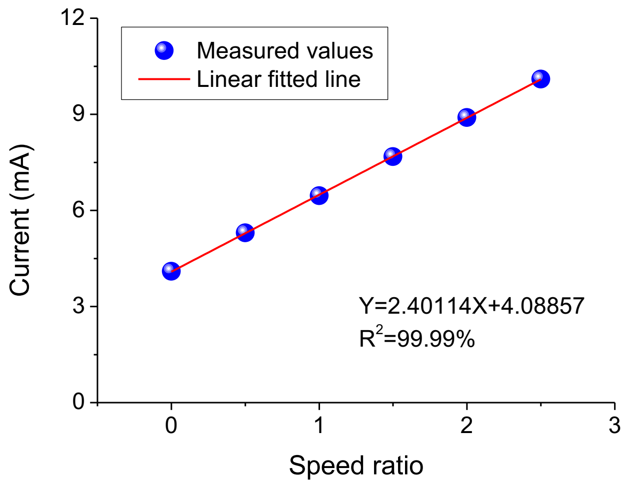

Figure 5 Calibration of the speed sensor

According to the aforementioned calibration results, it can be summarized that the proposed measurement system is suitable for measuring yarn twist and belt speed with excellent veracity and repeatability.

4.4 Yarn Measurement

Three cop yarns spun on three different spindles were produced for measurement. Before each testing, all samples were conditioned under standard laboratory conditions (20ºC ± 2ºC and 65% ± 2% relative humidity) for at least 24 hours, and all yarn properties measurement followed the methods as shown in Table 2. Yarn tenacity, evenness, hairiness and twist were important properties for the yarn.

Table 2 Yarn tests and standards

Properties	**Test Method**	**Test Apparatus**	**Procedure**
Tenacity	ASTM 2256-02	Uster Tensorapid 3	-Test speed:5m/min - Pretension: 0.5cN/tex - Test length: 500mm - Tests within: 50
Evenness	Uster Standard	Uster Tester 3 Evenness Convertor	-Test speed: 400m/min - Testing time: 1min - Tests within: 1
Twist	ISO 2061	Yarn Twist Tester	- Tests within: 10
Hairiness	ASTM D1423	Zweigle G566	- Test speed: 100m/min - Evaluation time: 1min - Tests within: 1

5 Results and Discussion

5.1 Yarn twist in OA zone

As shown in Figure 6, three cases of sinusoidal variation of the false twist with different frequencies were implemented, and the corresponding twist redistributions in OA zone were examined and compared with theoretical calculations. It can be found that the predicted curves generally follow a similar trend to the experimental data, despite some deviations are found with CV about 10% to 15%, implying that simulated yarn twist in OA zone matches well with actual data.

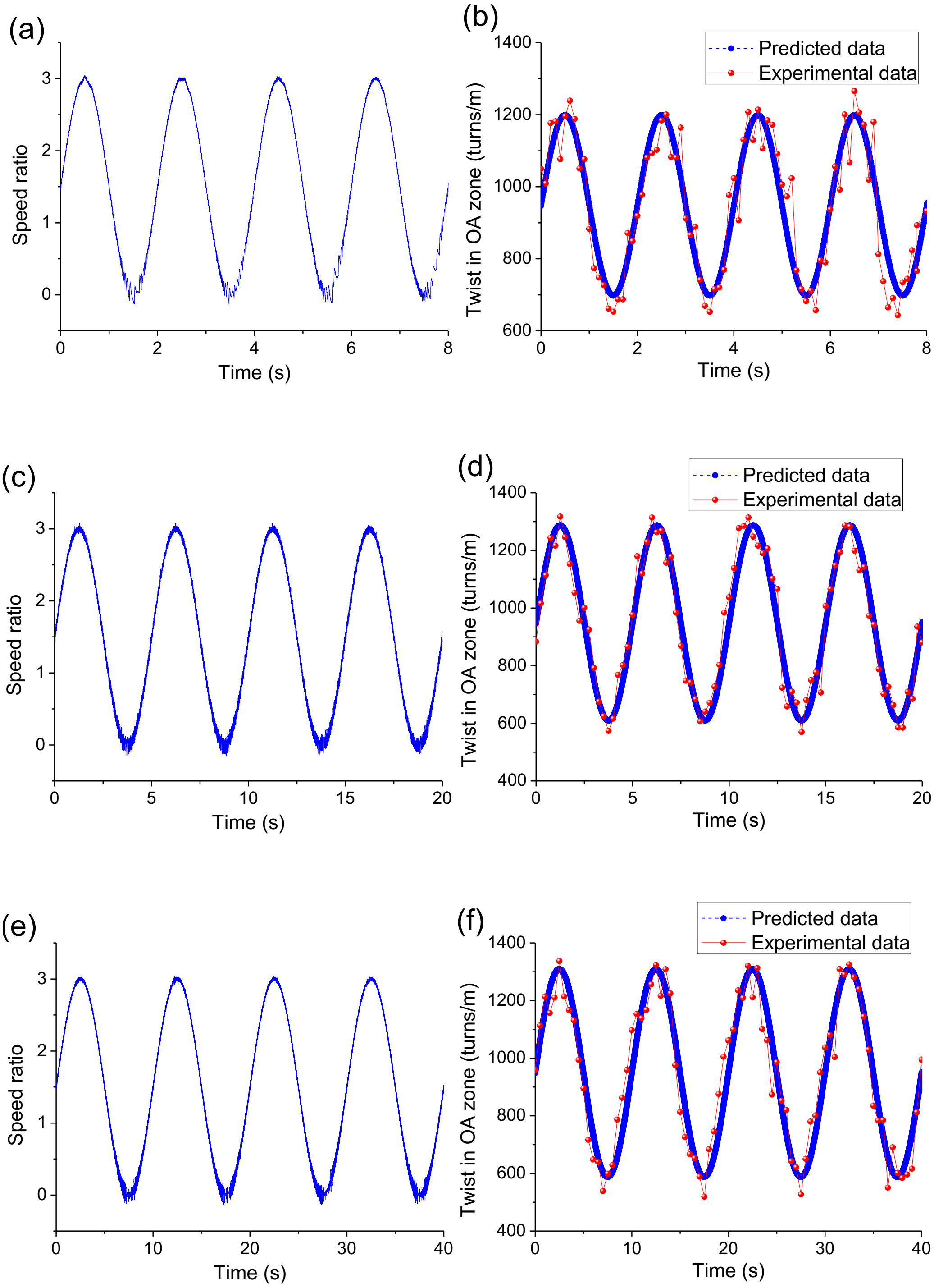

Figure 6 Sinusoidal variation of the false twist and comparison of experimental data against predicted data in OA zone

(a) Speed ratio changes periodically from 0 to 3 with period 2s; (b) The corresponding twist change in OA zone; (c) Speed ratio changes periodically from 0 to 3 with period 5s; (d) The corresponding twist change in OA zone; (e) Speed ratio changes periodically from 0 to 3 with period 10s; (f) The corresponding twist change in OA zone.

5.2 Measured yarn properties and final yarn twist

The properties of modified yarns with and without belt speed variations as well as conventional yarns are presented in Table 3. By comparing the properties of the modified yarn with that of conventional ring yarn with normal twist factor of 3.6, the modified yarn with 11.1% twist reduction apparently outweighed the conventional yarn in hairiness and has slight improvements in minimum tenacity, thin places (-40%), and thick places (+50%); whereas the mean tenacity, evenness, neps (+140%) is lightly worse than that of the corresponding ring yarn. Compared with the conventional ring yarn with the same twist factor, the optimized yarn has 0.74 cN/Tex higher in mean tenacity, 1.18 cN/Tex higher in minimum tenacity as well as much less hairiness.

Four yarns with period 5 seconds and periodic variation of the belt speed of 10%, 20%, 30% and 40% were produced to study the effect of variation of false twist on yarn performances, as listed in Table 3. Within 30% periodic variation of false twist, the yarn properties were not significantly affected. When the variation increased to 40%, the mean tenacity and minimum tenacity of the sample were decreased by 0.39, and 0.65 cN/Tex, respectively, and the neps of SB-40% were also increased by 10.08%.

Table 3 Measured properties of conventional yarns and yarns with and without belt speed variations

Yarn code	Tenacity (cN/Tex) [cv%]	Mini. Tenacity	Evenness CVm% [cv%]	Thin places (-40%) [cv%]	Thick places (+50%) [cv%]	Neps (+140%) [cv%]	Twist (tpm)	Hairiness (S3) [cv%]
Conv TF3.6	17.59 [7.50]	14.23	12.71 [1.23]	110 [7.27]	34 [29.85]	224 [14.75]	892 [8.38]	1321 [27.76]
Conv TF3.2	16.16 [5.80]	13.10	12.93 [1.11]	114 [23.25]	30 [7.53]	215 [17.84]	793 [7.37]	1611 [26.76]
SB-TF3.2	16.90 [7.52]	14.28	12.82 [2.84]	104 [13.87	21 [31.23]	248 [6.15]	789 [8.32	846 [3.93]

				]			]	
SB-10%	16.89 [6.76]	14.45	12.82 [0.95]	113 [11.65]	28 [22.96]	245 [9.91]	782 [8.30]	758 [0.37]
SB-20%	16.90 [5.81]	14.71	12.85 [0.79]	108 [2.34]	24 [7.22]	248 [16.32]	790 [9.23]	794 [7.66]
SB-30%	16.75 [5.22]	14.13	12.86 [0.72]	108 [30.92]	33 [34.95]	250 [5.29]	786 [9.20]	845 [1.67]
SB-40%	16.51 [7.65]	13.63	12.74 [0.67]	108 [20.06]	22 [11.27]	273 [9.29]	792 [8.10]	793 [4.82]

6 Simulation

The dimensionless model shows that lengths of divided zone path, false twist, belt properties etc influence on the twist redistribution. In order to fully evaluate the twist variation, a series of numerical simulations are carried out in this section. Among the twist distribution in three zones, yarn twists in zone OA and BC are of particular interests since they have large influence on yarn structure and properties.

6.1 Twist redistributions in three zones

The parameters used for simulation below are $\overline{N_b}=5$, λ=0.2, η=0.7, k=0.6, $\overline{l_1}=3.75$, $\overline{l_2}=20-\overline{l_1}$, unless otherwise stated. Figure 7 shows the results of twist redistribution in three zones under the condition of $\overline{\Delta N_b}=0.2\overline{N_b}$, $\overline{f}=0.15$. As might be predicted that, yarn twist in three zones varies periodically with the oscillation frequency of the false twist, but the phase angle and amplitude differ. The amplitude of $\overline{\mathbf{T_1}}$ can be nearly quarter that of the original twist oscillation, and the amplitude downstream the false-twister further attenuated as the yarn passes from one zone to the next. This is because the dwell time of the yarn in these zones is greater than the oscillation period.

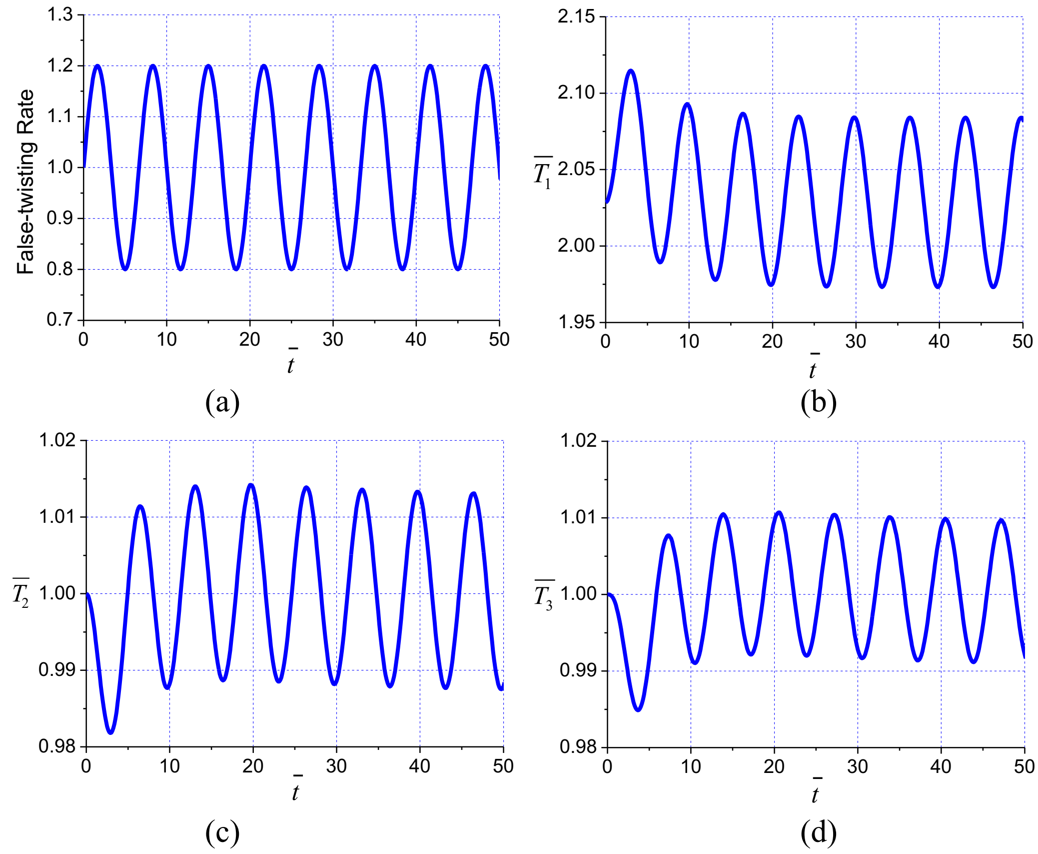

Figure 7 Twist changes in three zones by sinusoidal variation of false twist

6.2 Effect of system parameters on amplitudes of $\overline{\mathbf{T}}_1$ and $\overline{\mathbf{T}}_3$

Figure 8 shows the effect of oscillation frequency, false-twister position, and belt properties on the amplitudes of the twist in zone OA and BC. As the frequency increases, the twist oscillation becomes more and more damped. It can be seen from Figure 9(a, c) that at a higher $\bar{f}$ value of 0.25 and $\bar{l}_1$ of 3.75, the amplitudes of $\overline{\mathbf{T}}_1$ and $\overline{\mathbf{T}}_3$ are only 0.033 and 0.004, respectively. Besides, false-twister position has a certain influence on twist variation in zone OA. As the $\bar{l}_1$ increases, the amplitude of $\overline{\mathbf{T}}_1$ decreases, while the amplitude of $\overline{\mathbf{T}}_3$ raise sharply at low frequency rate and stably at high frequency rate. Nevertheless, the belt properties also affect twist changes in three zones; however the effect is small in high frequency rate.

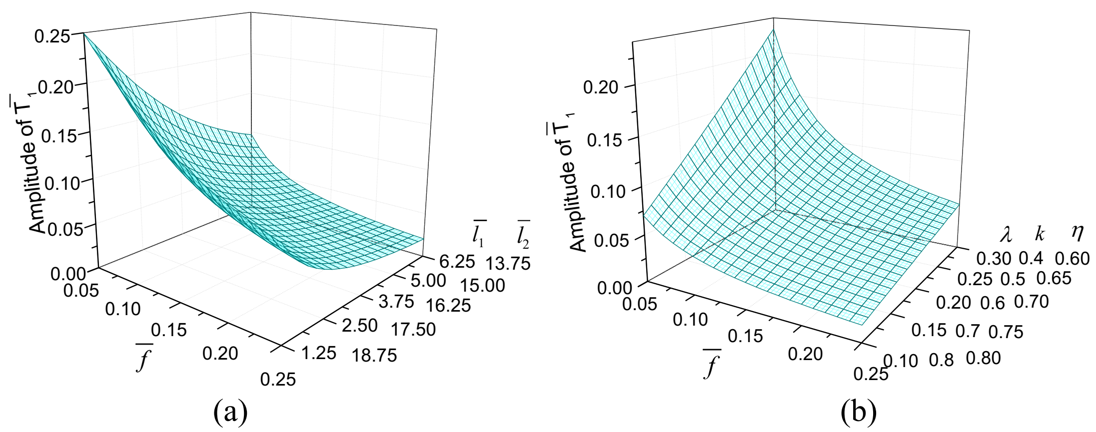

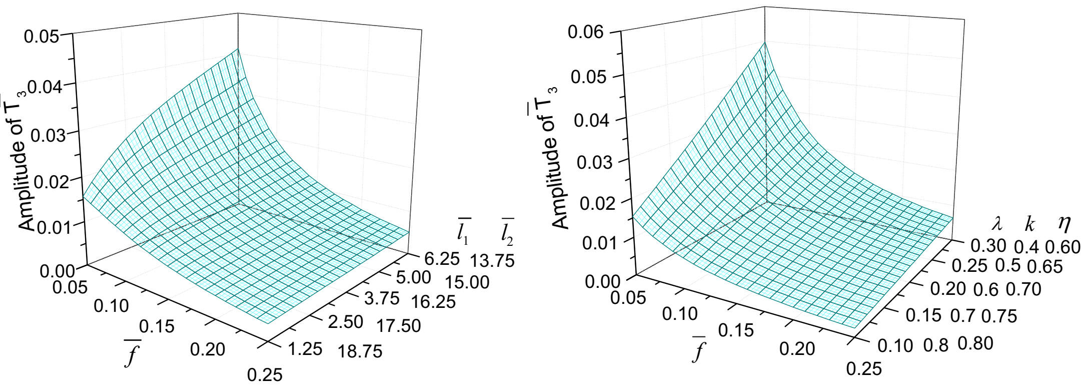

(c) (d)

Figure 8 The effect of $\overline{f}$, $\overline{l}_1$ and belt properties on the amplitude of $\overline{\mathbf{T}}_1$ and $\overline{\mathbf{T}}_3$

Practically, the vibration frequency (in Hz) of friction-belt transverse motion is the rate in single digits, and the vibration frequencies of belt torsional and longitudinal motion are at least one order of magnitude higher than that of transverse vibration, and therefore the effect of friction-belt vibration on yarn twist variation in three zones is limited. On the other hand, the periodic variation of yarn diameter due to yarn unevenness is a promising factor that causes large twist variation. Take cotton spinning and wool spinning for example. The typical wavelengths of cotton-like fibre (33 mm) and wool-like fibre (66 mm) are 89 mm and 198 mm, respectively. The corresponding $\overline{f}$ values are 0.225 and 0.101, respectively. Thus, the variation amplitudes of $\overline{\mathbf{T}}_1$ and $\overline{\mathbf{T}}_3$ are 0.063 and 0.005, respectively, for cotton-like fibre at the diameter variation of 15%, $\overline{l}_1$ of 2.5, and λ of 0.3; while the variation amplitudes of $\overline{\mathbf{T}}_1$ and $\overline{\mathbf{T}}_3$ for wool-like fibre reach as high as 0.133 and 0.016 at the same condition. Hence, the twist variation is more serious in wool-like yarn than that of cotton-like yarn.

7 Conclusions

This paper describes the effects of variations of false twist on process stability and resultant yarn quality in a modified ring spinning process. Although several basic simplifying assumptions have been necessary in order to make the analysis manageable, the findings have given a clear indication of the significant twist levels that can develop in the zones of the machine. Since twist in these zones can have a marked effect on the quality of the end-product, these results are of some practical significance. It has been proved by the experiment that within 30% periodic variation in false twist, the yarn properties were not significantly affected. In another words, the current configuration and system parameters are stable and robust as well as have a high tolerance for twist variations. From simulation, it has been demonstrated that belt oscillation has little effect on twist variation and wool-like fibre is easier to cause large twist variation in spinning process than that of cotton-like fiber at the same condition. At the least, the results should give rise to a better comprehending of the mechanism of false-twister adopted in a ring spinning frame and provide method of calculating the practical levels of twist control required to reduce certain remarkable yarn faults.

Acknowledgment

This research was funded in part through a research grant from the Research Grants

Council of the Hong Kong Special Administrative Region, China (Project No: B-Q35S) and a postgraduate scholarship by the Hong Kong Polytechnic University.

Appendix

1.Step function change in rotational speed of the false-twister

A step function change of false twist amount ΔN_b at time t_0 is assumed.

False Twist in Zone OA

When $t \le t_0$, yarn false twist in zone OA is

$$T_1 = \frac{\lambda N_b}{\eta v} \tag{A1}$$

When $t > t_0$, the turns gained by moving belt are $\lambda\left(N_b + \Delta N_b\right)dt$, turns lost through the belt are $\eta T_1 v dt$, therefore, the net twists gained are $dT_1 = \frac{\lambda\left(N_b + \Delta N_b\right) - \eta T_1 v}{l_1} dt$, integration of which together with the initial condition gives

$$T_1 = \frac{1}{\eta v}\left(\lambda\left(N_b + \Delta N_b\right) - \left(\lambda\left(N_b + \Delta N_b\right) - \eta v T_1 |_{t=t_0}\right) \exp\left(-\frac{\eta v}{l_1}(t - t_0) \right) \right) \tag{A2}$$

False Twist in Zone AB

When $t \le t_0$, yarn false twist in zone AB is

$$T_2 = 0 \tag{A3}$$

When $t > t_0$, the turns passing through the belt from Zone OA are $\eta T_1 v dt$, the negative turns inserted by the moving belt are $-\lambda\left(N_b + \Delta N_b\right)dt$, the turns passing through the traveler are $T_2 v dt$, therefore, the net twists gained are $dT_2 = \frac{\eta T_1 v - \lambda\left(N_b + \Delta N_b\right) - T_2 v}{l_2} dt$, integration of which together with the initial condition gives

$$T_2 = T_2 |_{t=t_0} \exp\left(-\frac{v}{l_2}(t - t_0) \right) - \frac{\lambda\left(N_b + \Delta N_b\right) - \eta v T_1 |_{t=t_0}}{v} \frac{l_1}{l_1 - \eta l_2} \left(\exp\left(-\frac{\eta v}{l_1}(t - t_0) \right) - \exp\left(-\frac{v}{l_2}(t - t_0) \right) \right) \tag{A4}$$

False Twist in Zone BC

When $t \le t_0$, yarn false twist in zone BC is

$$T_3 = 0 \tag{A5}$$

When $t > t_0$, the turns passing through the traveler from zone AB are $T_2 v dt$, the turns wound onto the bobbin are $T_3 v dt$, therefore, the net twists gained are $dT_3 = \frac{T_2 v - T_3 v}{l_3} dt$, integration of which together with the initial condition gives

$$T_3 = T_3\,|_{t=t_0}\exp\left(-\frac{v}{l_3}(t-t_0)\right)+\frac{l_2}{l_2-l_3}T_2\,|_{t=t_0}\left(\exp\left(-\frac{v}{l_2}(t-t_0)\right)-\exp\left(-\frac{v}{l_3}(t-t_0)\right)\right)$$
$$-\frac{\lambda\left(N_b+\Delta N_b\right)-\eta v T_1\,|_{t=t_0}}{v}\frac{l_1}{\left(l_1-\eta l_2\right)\left(l_1-\eta l_3\right)\left(l_2-l_3\right)} \tag{A6}$$
$$\left(l_1\left(l_2-l_3\right)\exp\left(-\frac{\eta v}{l_1}(t-t_0)\right)-l_2\left(l_1-\eta l_3\right)\exp\left(-\frac{v}{l_2}(t-t_0)\right)+l_3\left(l_1-\eta l_2\right)\exp\left(-\frac{v}{l_3}(t-t_0)\right)\right)$$

Therefore, yarn total twists in each zone can be expressed by the

$$\mathbf{T_1} = \begin{cases} \dfrac{kN_t}{v}+\dfrac{\lambda N_b}{\eta v} & ,t \le t_0 \\ \dfrac{kN_t}{v}+\dfrac{1}{\eta v}\left(\lambda\left(N_b+\Delta N_b\right)-\left(\lambda\left(N_b+\Delta N_b\right)-\eta v T_1\,|_{t=t_0}\right)\exp\left(-\dfrac{\eta v}{l_1}(t-t_0)\right)\right) & ,t > t_0 \end{cases} \tag{A7}$$

$$\mathbf{T_2} = \begin{cases} \dfrac{N_t}{v} & ,t \le t_0 \\ \dfrac{N_t}{v}+T_2\,|_{t=t_0}\exp\left(-\dfrac{v}{l_2}(t-t_0)\right)-\dfrac{\lambda\left(N_b+\Delta N_b\right)-\eta v T_1\,|_{t=t_0}}{v} & \\ \dfrac{l_1}{l_1-\eta l_2}\left(\exp\left(-\dfrac{\eta v}{l_1}(t-t_0)\right)-\exp\left(-\dfrac{v}{l_2}(t-t_0)\right)\right) & ,t > t_0 \end{cases} \tag{A8}$$

$$\mathbf{T_3} = \begin{cases} \dfrac{N_t}{v} & ,t \le t_0 \\ \dfrac{N_t}{v}+T_3\,|_{t=t_0}\exp\left(-\dfrac{v}{l_3}(t-t_0)\right)+\dfrac{l_2}{l_2-l_3}T_2\,|_{t=t_0}\left(\exp\left(-\dfrac{v}{l_2}(t-t_0)\right)-\exp\left(-\dfrac{v}{l_3}(t-t_0)\right)\right) & \\ -\dfrac{\lambda\left(N_b+\Delta N_b\right)-\eta v T_1\,|_{t=t_0}}{v}\dfrac{l_1}{\left(l_1-\eta l_2\right)\left(l_1-\eta l_3\right)\left(l_2-l_3\right)} & ,t > t_0 \\ \left(l_1\left(l_2-l_3\right)\exp\left(-\dfrac{\eta v}{l_1}(t-t_0)\right)-l_2\left(l_1-\eta l_3\right)\exp\left(-\dfrac{v}{l_2}(t-t_0)\right)+l_3\left(l_1-\eta l_2\right)\exp\left(-\dfrac{v}{l_3}(t-t_0)\right)\right) & \end{cases}$$

(A9)

Transforming equations (A7-A9) into the dimensionless form, one obtains

$$\overline{\mathbf{T_1}} = \begin{cases} k+\dfrac{\lambda\overline{N_b}}{\eta} & ,\bar{t} \le \overline{t_0} \\ k+\dfrac{1}{\eta}\left(\lambda\left(\overline{N_b}+\overline{\Delta N_b}\right)-\left(\lambda\left(\overline{N_b}+\overline{\Delta N_b}\right)-\eta\overline{T_1\,|_{t=t_0}}\right)\exp\left(-\dfrac{\eta}{\overline{l_1}}(\bar{t}-\overline{t_0})\right)\right) & ,\bar{t} > \overline{t_0} \end{cases} \tag{A10}$$

$$\overline{\mathbf{T_2}} = \begin{cases} 1 & ,\bar{t} \le \overline{t_0} \\ 1+\overline{T_2\,|_{t=t_0}}\exp\left(-\dfrac{1}{\overline{l_2}}(\bar{t}-\overline{t_0})\right)-\left(\lambda\left(\overline{N_b}+\overline{\Delta N_b}\right)-\eta\overline{T_1\,|_{t=t_0}}\right) & \\ \dfrac{\overline{l_1}}{\overline{l_1}-\eta\overline{l_2}}\left(\exp\left(-\dfrac{\eta}{\overline{l_1}}(\bar{t}-\overline{t_0})\right)-\exp\left(-\dfrac{1}{\overline{l_2}}(\bar{t}-\overline{t_0})\right)\right) & ,\bar{t} > \overline{t_0} \end{cases} \tag{A11}$$

$$\overline{\mathbf{T}_3} = \begin{cases} 1 & ,\bar{t} \le \overline{t_0} \\ 1 + \overline{T_3 |_{t=t_0}} \exp\left(-\frac{1}{\overline{l_3}}(\bar{t} - \overline{t_0}) \right) + \frac{\overline{l_2}}{\overline{l_2} - 1} \overline{T_2 |_{t=t_0}} \left(\exp\left(-\frac{1}{\overline{l_2}}(\bar{t} - \overline{t_0}) \right) - \exp\left(-\frac{1}{\overline{l_3}}(\bar{t} - \overline{t_0}) \right) \right) & \\ -\left(\lambda\left(\overline{N_b} + \overline{\Delta N_b} \right) - \eta \overline{T_1 |_{t=t_0}} \right) \frac{\overline{l_1}}{\left(\overline{l_1} - \eta \overline{l_2} \right)\left(\overline{l_1} - \eta \right)\left(\overline{l_2} - 1 \right)} & ,\bar{t} > \overline{t_0} \\ \left(\overline{l_1}\left(\overline{l_2} - 1 \right) \exp\left(-\frac{\eta}{\overline{l_1}}(\bar{t} - \overline{t_0}) \right) - \overline{l_2}\left(\overline{l_1} - \eta \right) \exp\left(-\frac{1}{\overline{l_2}}(\bar{t} - \overline{t_0}) \right) + \left(\overline{l_1} - \eta \overline{l_2} \right) \exp\left(-(\bar{t} - \overline{t_0}) \right) \right) & \end{cases} \quad \text{(A12)}$$

where $\bar{t} = \frac{vt}{l_3}$, $\overline{t_0} = \frac{vt_0}{l_3}$, $\overline{l_1} = \frac{l_1}{l_3}$, $\overline{l_2} = \frac{l_2}{l_3}$, $\overline{T_1} = \frac{vT_1}{N_t}$, $\overline{T_2} = \frac{vT_2}{N_t}$, $\overline{T_3} = \frac{vT_3}{N_t}$, $\overline{N_b} = \frac{N_b}{N_t}$, $\overline{\Delta N_b} = \frac{\Delta N_b}{N_t}$

2.Rectangular function change

In order to study this situation, a change of false twist amount ΔN_b at a short period Δt is assumed.

False Twist in Zone OA

When $t \le t_0$, yarn false twist in zone OA is

$$T_1 = \frac{\lambda N_b}{\eta v} \quad \text{(A13)}$$

When $t_0 < t \le t_0 + \Delta t$, the turns gained by the moving belt are $\lambda\left(N_b + \Delta N_b\right)dt$, the turns lost through the belt are $\eta T_1 v dt$, therefore, the net twists gained are $dT_1 = \frac{\lambda\left(N_b + \Delta N_b\right) - \eta T_1 v}{l_1} dt$, integration of which together with the initial condition gives

$$T_1 = \frac{1}{\eta v}\left(\lambda\left(N_b + \Delta N_b\right) - \left(\lambda\left(N_b + \Delta N_b\right) - \eta v T_1 |_{t=t_0} \right) \exp\left(-\frac{\eta v}{l_1}(t - t_0) \right) \right) \quad \text{(A14)}$$

When $t > t_0 + \Delta t$, the turns gained by the moving belt are $\lambda N_b dt$, the turns lost through the belt are $\eta T_1 v dt$, the net twists gained are $dT_1 = \frac{\lambda N_b - \eta T_1 v}{l_1} dt$, integration of which together with the initial condition , gives

$$T_1 = \frac{1}{\eta v}\left(\lambda N_b - \left(\lambda N_b - \eta v T_1 |_{t=t_0+\Delta t} \right) \exp\left(-\frac{\eta v}{l_1}(t - t_0 - \Delta t) \right) \right) \quad \text{(A15)}$$

False Twist in Zone AB

When $t \le t_0$, yarn false twist in zone AB is

$$T_2 = 0 \quad \text{(A16)}$$

When $t_0 < t \le t_0 + \Delta t$, the turns passing through the belt from Zone OA are $\eta T_1 v dt$, the negative turns inserted by the moving belt are $-\lambda\left(N_b + \Delta N_b\right)dt$, the turns passing through the traveler are $T_2 v dt$, therefore, the net twists gained are

$dT_2 = \dfrac{\eta T_1 v - \lambda\left(N_b + \Delta N_b\right) - T_2 v}{l_2} dt$, integration of which together with the initial condition in equation (19), gives

$$T_2 = T_2\,|_{t=t_0} \exp\left(-\frac{v}{l_2}(t-t_0) \right) - \frac{\lambda\left(N_b + \Delta N_b\right) - \eta v T_1\,|_{t=t_0}}{v} \frac{l_1}{l_1 - \eta l_2} \left(\exp\left(-\frac{\eta v}{l_1}(t-t_0) \right) - \exp\left(-\frac{v}{l_2}(t-t_0) \right) \right)$$

(A17)

When $t > t_0 + \Delta t$, the turns passing through the belt from Zone OA be $\eta T_1 v dt$, the negative turns inserted by the moving belt be $-\lambda N_b dt$, the turns passing through the traveler be $T_2 v dt$, therefore, the net twists gained be $dT_2 = \dfrac{\eta T_1 v - \lambda N_b - T_2 v}{l_2} dt$., integration of which together with the initial condition, gives

$$T_2 = T_2\,|_{t=t_0+\Delta t} \exp\left(-\frac{v}{l_2}(t-t_0-\Delta t) \right) - \frac{\lambda N_b - \eta v T_1\,|_{t=t_0+\Delta t}}{v} \frac{l_1}{l_1 - \eta l_2} \left(\exp\left(-\frac{\eta v}{l_1}(t-t_0-\Delta t) \right) - \exp\left(-\frac{v}{l_2}(t-t_0-\Delta t) \right) \right) \quad \text{(A18)}$$

False Twist in Zone BC

When $t \le t_0$, yarn false twist in zone BC is

$$T_3 = 0 \quad \text{(A19)}$$

When $t_0 < t \le t_0 + \Delta t$, the turns passing through the traveler from zone AB are $T_2 v dt$, the turns wound onto the bobbin are $T_3 v dt$, therefore, the net twists gained are $dT_3 = \dfrac{T_2 v - T_3 v}{l_3} dt$, integration of which together with the initial condition, gives

$$\begin{aligned} T_3 = {} & T_3\,|_{t=t_0} \exp\left(-\frac{v}{l_3}(t-t_0) \right) + \frac{l_2}{l_2 - l_3} T_2\,|_{t=t_0} \left(\exp\left(-\frac{v}{l_2}(t-t_0) \right) - \exp\left(-\frac{v}{l_3}(t-t_0) \right) \right) \\ & - \frac{\lambda\left(N_b + \Delta N_b\right) - \eta v T_1\,|_{t=t_0}}{v} \frac{l_1}{\left(l_1 - \eta l_2\right)\left(l_1 - \eta l_3\right)\left(l_2 - l_3\right)} \\ & \left(l_1\left(l_2 - l_3\right)\exp\left(-\frac{\eta v}{l_1}(t-t_0) \right) - l_2\left(l_1 - \eta l_3\right)\exp\left(-\frac{v}{l_2}(t-t_0) \right) + l_3\left(l_1 - \eta l_2\right)\exp\left(-\frac{v}{l_3}(t-t_0) \right) \right) \end{aligned} \quad \text{(A20)}$$

When $t > t_0 + \Delta t$, the turns passing through the traveler from Zone AB are $T_2 v dt$, the turns wound onto the bobbin are $T_3 v dt$, therefore, the net twists gained are $dT_3 = \dfrac{T_2 v - T_3 v}{l_3} dt$, integration of which together with the initial condition, gives

$$
\begin{aligned}
T_3 &= T_3|_{t=t_0+\Delta t}\exp\left(-\frac{v}{l_3}(t-t_0-\Delta t)\right) \\
&+\frac{l_2}{l_2-l_3}T_2|_{t=t_0+\Delta t}\left(\exp\left(-\frac{v}{l_2}(t-t_0-\Delta t)\right)-\exp\left(-\frac{v}{l_3}(t-t_0-\Delta t)\right)\right) \\
&-\frac{\lambda N_b-\eta v T_1|_{t=t_0+\Delta t}}{v}\frac{l_1}{(l_1-\eta l_2)(l_1-\eta l_3)(l_2-l_3)} \\
&\left(\begin{aligned}&l_1(l_2-l_3)\exp\left(-\frac{\eta v}{l_1}(t-t_0-\Delta t)\right)-l_2(l_1-\eta l_3)\exp\left(-\frac{v}{l_2}(t-t_0-\Delta t)\right)\\&+l_3(l_1-\eta l_2)\exp\left(-\frac{v}{l_3}(t-t_0-\Delta t)\right)\end{aligned}\right)
\end{aligned}
\tag{A21}
$$

Therefore, yarn total twists in each zone can be expressed by the

$$
\mathbf{T_1}=\begin{cases}
\dfrac{kN_t}{v}+\dfrac{\lambda N_b}{\eta v} & ,t\le t_0 \\
\dfrac{kN_t}{v}+\dfrac{1}{\eta v}\left(\lambda(N_b+\Delta N_b)-\left(\lambda(N_b+\Delta N_b)-\eta v T_1|_{t=t_0}\right)\exp\left(-\dfrac{\eta v}{l_1}(t-t_0)\right)\right) & ,t_0<t\le t_0+\Delta t \\
\dfrac{kN_t}{v}+\dfrac{1}{\eta v}\left(\lambda N_b-\left(\lambda N_b-\eta v T_1|_{t=t_0+\Delta t}\right)\exp\left(-\dfrac{\eta v}{l_1}(t-t_0-\Delta t)\right)\right) & ,t>t_0+\Delta t
\end{cases}
\tag{A22}
$$

$$
\mathbf{T_2}=\begin{cases}
\dfrac{N_t}{v} & ,t\le t_0 \\
\begin{aligned}&\dfrac{N_t}{v}+T_2|_{t=t_0}\exp\left(-\dfrac{v}{l_2}(t-t_0)\right)-\dfrac{\lambda(N_b+\Delta N_b)-\eta v T_1|_{t=t_0}}{v}\\&\dfrac{l_1}{l_1-\eta l_2}\left(\exp\left(-\dfrac{\eta v}{l_1}(t-t_0)\right)-\exp\left(-\dfrac{v}{l_2}(t-t_0)\right)\right)\end{aligned} & ,t_0<t\le t_0+\Delta t \\
\begin{aligned}&\dfrac{N_t}{v}+T_2|_{t=t_0+\Delta t}\exp\left(-\dfrac{v}{l_2}(t-t_0-\Delta t)\right)-\dfrac{\lambda N_b-\eta v T_1|_{t=t_0+\Delta t}}{v}\\&\dfrac{l_1}{l_1-\eta l_2}\left(\exp\left(-\dfrac{\eta v}{l_1}(t-t_0-\Delta t)\right)-\exp\left(-\dfrac{v}{l_2}(t-t_0-\Delta t)\right)\right)\end{aligned} & ,t>t_0+\Delta t
\end{cases}
\tag{A23}
$$

$$
\mathbf{T_3}=\begin{cases}
\dfrac{N_t}{v} & ,t\le t_0\\[2ex]
\dfrac{N_t}{v}+T_3|_{t=t_0}\exp\left(-\dfrac{v}{l_3}(t-t_0)\right)+\dfrac{l_2}{l_2-l_3}T_2|_{t=t_0}\left(\exp\left(-\dfrac{v}{l_2}(t-t_0)\right)-\exp\left(-\dfrac{v}{l_3}(t-t_0)\right)\right)\\
-\dfrac{\lambda\left(N_b+\Delta N_b\right)-\eta v T_1|_{t=t_0}}{v}\dfrac{l_1}{\left(l_1-\eta l_2\right)\left(l_1-\eta l_3\right)\left(l_2-l_3\right)} & ,t_0<t\le t_0+\Delta t\\
\left(l_1\left(l_2-l_3\right)\exp\left(-\dfrac{\eta v}{l_1}(t-t_0)\right)-l_2\left(l_1-\eta l_3\right)\exp\left(-\dfrac{v}{l_2}(t-t_0)\right)+l_3\left(l_1-\eta l_2\right)\exp\left(-\dfrac{v}{l_3}(t-t_0)\right)\right)\\
\dfrac{N_t}{v}+T_3|_{t=t_0+\Delta t}\exp\left(-\dfrac{v}{l_3}(t-t_0-\Delta t)\right)+\dfrac{l_2}{l_2-l_3}T_2|_{t=t_0+\Delta t}\left(\exp\left(-\dfrac{v}{l_2}(t-t_0-\Delta t)\right)-\exp\left(-\dfrac{v}{l_3}(t-t_0-\Delta t)\right)\right)\\
-\dfrac{\lambda N_b-\eta v T_1|_{t=t_0+\Delta t}}{v}\dfrac{l_1}{\left(l_1-\eta l_2\right)\left(l_1-\eta l_3\right)\left(l_2-l_3\right)} & ,t>t_0+\Delta t\\
\left(l_1\left(l_2-l_3\right)\exp\left(-\dfrac{\eta v}{l_1}(t-t_0-\Delta t)\right)-l_2\left(l_1-\eta l_3\right)\exp\left(-\dfrac{v}{l_2}(t-t_0-\Delta t)\right)+l_3\left(l_1-\eta l_2\right)\exp\left(-\dfrac{v}{l_3}(t-t_0-\Delta t)\right)\right)
\end{cases}
\tag{A24}
$$

Transforming equations (A22-A24) into the dimensionless form, one obtains

$$
\overline{\mathbf{T_1}}=\begin{cases}
k+\dfrac{\lambda\overline{N_b}}{\eta} & ,\bar{t}\le\overline{t_0}\\
k+\dfrac{1}{\eta}\left(\lambda\left(\overline{N_b}+\overline{\Delta N_b}\right)-\left(\lambda\left(\overline{N_b}+\overline{\Delta N_b}\right)-\eta\overline{T_1|_{t=t_0}}\right)\exp\left(-\dfrac{\eta}{\overline{l_1}}(\bar{t}-\overline{t_0})\right)\right) & ,\overline{t_0}<\bar{t}\le\overline{t_0+\Delta t}\\
k+\dfrac{1}{\eta}\left(\lambda\overline{N_b}-\left(\lambda\overline{N_b}-\eta\overline{T_1|_{t=t_0+\Delta t}}\right)\exp\left(-\dfrac{\eta}{\overline{l_1}}(\bar{t}-\overline{t_0}-\overline{\Delta t})\right)\right) & ,\bar{t}>\overline{t_0+\Delta t}
\end{cases}
\tag{A25}
$$

$$\overline{\mathbf{T_2}} = \begin{cases} 1 & ,\bar{t} \le \overline{t_0} \\ 1+\overline{T_2|_{t=t_0}}\exp\left(-\frac{1}{\overline{l_2}}(\bar{t}-\overline{t_0})\right)-\left(\lambda\left(\overline{N_b}+\overline{\Delta N_b}\right)-\eta\overline{T_1|_{t=t_0}}\right) \\ \frac{\overline{l_1}}{\overline{l_1}-\eta\overline{l_2}}\left(\exp\left(-\frac{\eta}{\overline{l_1}}(\bar{t}-\overline{t_0})\right)-\exp\left(-\frac{1}{\overline{l_2}}(\bar{t}-\overline{t_0})\right)\right) & ,\overline{t_0}<\bar{t}\le\overline{t_0}+\overline{\Delta t} \\ 1+\overline{T_2|_{t=t_0+\Delta t}}\exp\left(-\frac{1}{\overline{l_2}}(\bar{t}-\overline{t_0}-\overline{\Delta t})\right)-\left(\lambda\overline{N_b}-\eta\overline{T_1|_{t=t_0+\Delta t}}\right) \\ \frac{\overline{l_1}}{\overline{l_1}-\eta\overline{l_2}}\left(\exp\left(-\frac{\eta}{\overline{l_1}}(\bar{t}-\overline{t_0}-\overline{\Delta t})\right)-\exp\left(-\frac{1}{\overline{l_2}}(\bar{t}-\overline{t_0}-\overline{\Delta t})\right)\right) & ,\bar{t}>\overline{t_0}+\overline{\Delta t} \end{cases} \quad \text{(A26)}$$

$$\overline{\mathbf{T_3}} = \begin{cases} 1 & ,\bar{t} \le \overline{t_0} \\ 1+\overline{T_3|_{t=t_0}}\exp\left(-(\bar{t}-\overline{t_0})\right)+\frac{\overline{l_2}}{\overline{l_2}-1}\overline{T_2|_{t=t_0}}\left(\exp\left(-\frac{1}{\overline{l_2}}(\bar{t}-\overline{t_0})\right)-\exp\left(-(\bar{t}-\overline{t_0})\right)\right) \\ -\left(\lambda\left(\overline{N_b}+\overline{\Delta N_b}\right)-\eta\overline{T_1|_{t=t_0}}\right)\frac{\overline{l_1}}{\left(\overline{l_1}-\eta\overline{l_2}\right)\left(\overline{l_1}-\eta\right)\left(\overline{l_2}-1\right)} & ,\overline{t_0}<\bar{t}\le\overline{t_0}+\overline{\Delta t} \\ \left(\overline{l_1}\left(\overline{l_2}-1\right)\exp\left(-\frac{\eta}{\overline{l_1}}(\bar{t}-\overline{t_0})\right)-\overline{l_2}\left(\overline{l_1}-\eta\right)\exp\left(-\frac{1}{\overline{l_2}}(\bar{t}-\overline{t_0})\right)+\left(\overline{l_1}-\eta\overline{l_2}\right)\exp\left(-(\bar{t}-\overline{t_0})\right)\right) \\ 1+\overline{T_3|_{t=t_0+\Delta t}}\exp\left(-(\bar{t}-\overline{t_0}-\overline{\Delta t})\right)+\frac{\overline{l_2}}{\overline{l_2}-1}\overline{T_2|_{t=t_0+\Delta t}}\left(\exp\left(-\frac{1}{\overline{l_2}}(\bar{t}-\overline{t_0}-\overline{\Delta t})\right)-\exp\left(-(\bar{t}-\overline{t_0}-\overline{\Delta t})\right)\right) \\ -\left(\lambda\overline{N_b}-\eta\overline{T_1|_{t=t_0+\Delta t}}\right)\frac{\overline{l_1}}{\left(\overline{l_1}-\eta\overline{l_2}\right)\left(\overline{l_1}-\eta\right)\left(\overline{l_2}-1\right)} & ,\bar{t}>\overline{t_0}+\overline{\Delta t} \\ \left(\overline{l_1}\left(\overline{l_2}-1\right)\exp\left(-\frac{\eta}{\overline{l_1}}(\bar{t}-\overline{t_0}-\overline{\Delta t})\right)-\overline{l_2}\left(\overline{l_1}-\eta\right)\exp\left(-\frac{1}{\overline{l_2}}(\bar{t}-\overline{t_0}-\overline{\Delta t})\right)+\left(\overline{l_1}-\eta\overline{l_2}\right)\exp\left(-(\bar{t}-\overline{t_0}-\overline{\Delta t})\right)\right) \end{cases}$$

(A27)

where $\bar{t}=\frac{vt}{l_3}$, $\overline{\Delta t}=\frac{v\Delta t}{l_3}$, $\overline{t_0}=\frac{vt_0}{l_3}$, $\overline{l_1}=\frac{l_1}{l_3}$, $\overline{l_2}=\frac{l_2}{l_3}$, $\overline{T_1}=\frac{vT_1}{N_t}$, $\overline{T_2}=\frac{vT_2}{N_t}$, $\overline{T_3}=\frac{vT_3}{N_t}$, $\overline{N_b}=\frac{N_b}{N_t}$

References

1. Hearle JWS, Grosberg P and Backer S. *Structural Mechanics of Fibers, Yarns, and Fabrics*. New

York: Wiley-Interscience, 1969, p.61.

2. Lawrence CA. *Advances in yarn spinning technology*. Cambridge: Woodhead Publishing Ltd, 2010, p.262.

3. Batra SK and Fraser WB. *Engineering fundamentals of ring spinning/twisting, over-end unwinding and two-for-one twisting in textile processes*. 1st ed. DEStech, 2015, p.1.

4. Guo Y, Feng J, Yin R, Wang XG, van der Sluijs M and Tao XM. Investigation and evaluation on fine Upland cotton blend yarns made by the modified ring spinning system. *Text Res J* 2015; 85: 1355-1366.

5. Chi PC, Ki LC and Tao XM. *Method of Industrially Producing Yarn at a Lower Twist Multiplier for Textile Products*. Patent 7,841,161 B2, USA, 2010.

6. Yang K, Tao XM, Xu BG and Lam J. Structure and properties of low twist short-staple singles ring spun yarns. *Text Res J* 2007; 77: 675-685.

7. Xu BG and Tao XM. Techniques for Torque Modification of Singles Ring Spun Yarns. *Text Res J* 2008; 78: 869-879.

8. Xu BG, Tao XM and Leung CS. A comparative study of cotton knitted fabrics and garments produced by the modified low twist and conventional ring yarns. *Fiber Polym* 2010; 11: 899-904.

9. Feng J, Xu BG and Tao XM. A Comparative Study of Finer Conventional and Modified Cotton Yarns and Their Resultant Woven Fabrics. *Fiber Polym* 2013; 14: 1899-1905.

10. Yin R, Tao XM and Xu BG. Mathematical Modeling of Yarn Dynamics in a Generalized Twisting System. *Sci Rep-Uk* 2016; 6: 24432.

11. Yin R and Gu HB. Numerical simulation of quasi-stationary ring spinning process linear elastic yarn. *Text Res J* 2011; 81: 22-27.

12. Yin R and Gu HB. Accurate prediction of the ring-spinning equation in zero air drag based on homotopy perturbation method. *J Text I* 2011; 102: 763-766.

13. Yin R, Liu Y and Gu HB. The Effect of Ring-spinning Parameters: Result from Theoretical Model. In: *Proceedings Of the Second International Conference on Advanced Textile Materials & Manufacturing Technology*, Yichang, China, 12 Nov-14 Nov 2010, paper no. 364, pp 530-534.

14. Fraser WB. On the Theory Of Ring Spinning. *Philos T Roy Soc A* 1993; 342: 439-468.

15. Xu BG and Tao XM. Integrated approach to dynamic analysis of yarn twist distribution in rotor spinning. *Text Res J* 2003; 73: 79-89.

16. Long JL, Xu BG and Tao XM. A Nonlinear Dynamic Model for Periodic Motion of Slender Thread line Structures. *Cmes-Comp Model Eng* 2011; 72: 273-297.

17. Lord PR and Rust JP. Fiber Assembly In Friction Spinning. *J Text I* 1991; 82: 465-478.

18. Lord PR and Rust JP. The Surface Of the Tail In Open-End Friction Spinning. *J Text I* 1990; 81: 100-103.

19. Lappage J. Self-Twist Spinning Of Yarns Of High Linear Density From Coarse Wools .1. Modified Repco Spinner And Some Properties Of St Yarns Of High Linear Density. *J Text I* 1978; 69: 17-23.

20. Lappage J. Self-Twist Spinning Of Yarns Of High Linear Density From Coarse Wools .2. Effects Of Fiber Diameter And Strand Linear Density Of Efficiency Of Twisting. *J Text I* 1978; 69: 24-31.

21. Lappage J. Self-Twist Spinning Of Yarns Of High Linear Density From Coarse Wools .3. Some Technological Implications. *J Text I* 1978; 69: 32-37.

22. Modelski TW. Repco Self-Twist Spinning. *Text I Ind* 1975; 13: 285-289.

23. Yu CW. Open-end spinning using air-jet twisting. *Text Res J* 1999; 69: 535-538.

24. Zeng YC and Yu CW. Numerical simulation of fiber motion in the nozzle of an air-jet spinning

machine. *Text Res J* 2004; 74: 117-122.
25. Fraser WB, Farnell L and Stump DM. Effect Of Yarn Nonuniformity on the Stability Of the Ring-Spinning Balloon. *P R Soc-Math Phys Sc* 1995; 449: 597-621.
26. Denton MJ. Twisting-Rate Variations In False-Twist Threadline .1. Background And Effect Of a Step Change In Twisting Rate. *J Text I* 1975; 66: 282-288.
27. Denton MJ. Development Of False Twist In Bulking. *J Text I* 1968; 59: 344-346.
28. Denton MJ. Twisting-Rate Variations In False-Twist Threadline .2. Effects Of a Rectangular-Pulse Transient Change And a Sinusoidal Variation In Twisting Rate. *J Text I* 1975; 66: 289-296.
29. Feng J, Xu BG and Tao XM. Dynamic measurement and modelling of flexible yarn dynamic behaviour on a moving cylindrical solid structure. *Meas Sci Technol* 2012; 23: 23-34.